Electronic structures of (In,Ga)As/GaAs quantum dot molecules made of dots with dissimilar sizes

Lixin He
Key Laboratory of Quantum Information, University of Science and Technology of China, Hefei, Anhui 230026, People's Republic of China

Alex Zunger
National Renewable Energy Laboratory, Golden, Colorado 80401, USA

(Received 8 August 2006; revised manuscript received 8 December 2006; published 26 February 2007)

Using single-particle pseudopotential and many-particle configuration interaction methods, we compare various physical quantities of (In,Ga)As/GaAS quantum dot molecules (QDM's) made of dissimilar dots (heteropolar QDM's) with QDM's made of identical dots (homopolar QDM's). The calculations show that the electronic structures of hetero-QDM's and homo-QDM's differ significantly at large interdot distance. In particular, (i) unlike those of homo-QDM's, the single-particle molecular orbitals of hetero-QDM's convert to dot-localized orbitals at large interdot distance. (ii) Consequently, in a hetero-QMD the bonding-antibonding splitting of molecular orbitals at large interdot distance is significantly larger than the electron hopping energy whereas for a homo-QDM, the bonding-antibonding splitting is very similar to the hopping energy. (iii) The asymmetry of the QDM increases significantly the double occupation for the two-electron ground states and therefore lowers the degree of entanglement of the two electrons.

DOI: 10.1103/PhysRevB.75.075330 PACS number(s): 73.22.Gk, 03.67.Mn, 85.35.−p

I. INTRODUCTION

Vertically coupled quantum dots[1,2] obtained via epitaxial growth provide a potential scheme for scalable nanostructures for quantum computing. In this scheme, two coupled quantum dots are used as a basic logic gate, via the entanglement of one exciton[3] or two electronic spins.[4] This proposal for gate operations requires knowledge of the detailed physical properties of the "quantum gate" made of two quantum dots. Significant progress has been recently made[5,6] using quantum dot molecules (QDM's) made of very large (~500–1000 Å) electrostatically confined dots. The limit of large quantum confinement, however, requires working with (200×30 Å^2) self-assembled QDM's. So far, most experiments on self-assembled QDM's are optical[3] and most theories are based on continuum models, such as effective mass approximations.[3] These simple models ignore or drastically simplify important real material properties such as strain, atomistic symmetries, crystal structural effects, band coupling, etc. Recent studies[7] show that simplification of such important effects may lead to qualitative changes in fundamental physics of the QDM's.

Previously, we have studied homopolar QDM's made of two identical quantum dots, using the single-particle pseudopotential method and many-particle configuration interaction method.[8,9] We have studied electron localization, the double occupation rate, and two-electron entanglement using a new formula for measuring the degree of entanglement formula for two *indistinguishable* fermions. We found that even geometrically identical dots in the QDM's lead to electronic asymmetry due to the strain effects. However, experimentally it is hard to control the shape, size, and compositions of individual dots within the QDM's, so, in practice, the QDM's are never made of identical dots. Actually, the top dots are tend to be larger than the bottom dots due to the strain effects.[1,2] Indeed, the measured difference in exciton energy due to dot-size difference is about 4 meV (Ref. 10) for two vertically coupled dots that are 20 nm apart. Sometimes, the two dots are intentionally grown differently so that they can be addressed separately.[11] To provide a quantitative comparison to experiments, considering the effects of asymmetry of quantum dots within the molecule, we studied QDM's made of (In,Ga)As/GaAS quantum dots of different sizes (heteropolar QDM's).

In this paper, we study systematically the electronic properties of hetero-QDM's, including their single-particle molecular orbitals, many-particle states, double occupation, and entanglement of two electrons, and compare them to those of homo-QDM's. We found that while at *short* interdot distance, the electronic properties of hetero-QDM's and homo-QDM's are similar, they differ significantly at *large* interdot distance. This difference may have substantial impact on the implementation of quantum gates.

II. METHODS

Figure 1 shows the geometry of a hetero-QDM, consisting a pair of 3-nm-tall InAs dots in the shape of truncated cones, grown on two-dimensional InAs wetting layers, embedded in a GaAs matrix. The interdot separation d is defined as the distance between the wetting layers of the top and bottom dots. We choose the base diameter of the top dots (labeled as α) to be 20 nm and that of the bottom dots (labeled as β) to be 19 nm, mimicking the fact that experimentally the top dots are slightly larger than the bottom dots.[1,2,10] The composition of the dots varies from $In_{0.5}Ga_{0.5}As$ at their bases to pure InAs at their top, as determined in Ref. 3. We denote the dot molecules made of dissimilar dots α and β as $M_{\alpha\beta}$. We also constructed the homo-QDM, consisting a pair of quantum dots γ, which have the average sizes and the same alloy

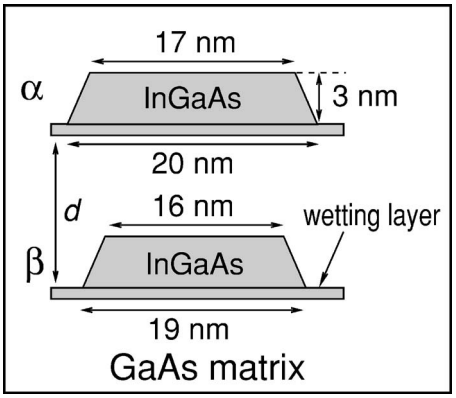

FIG. 1. The geometry used in this work for quantum dot molecules made of dissimilar dots. We denote the (isolated) top dot α and the (isolated) bottom dot β. Each dot has the shape of a truncated cone. The interdot distance is measured from wetting layer to wetting layer.

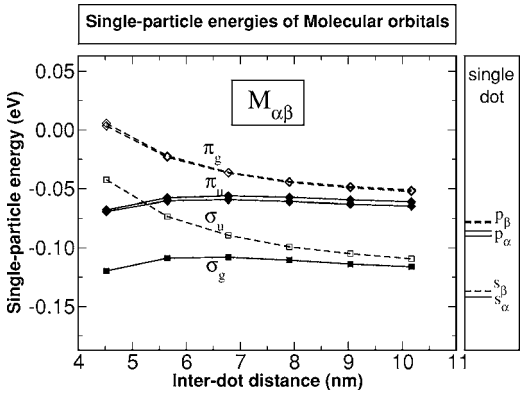

FIG. 2. Left panel: the single-particle energy levels of molecular orbitals vs interdot distance. Right panel: the electron single-particle energy levels of the isolated dots α and β.

compositions of dots α and β in the heteropolar dot molecule. We denote the homo-QDM as $M_{\gamma\gamma}$.

The single-particle energy levels and wave functions of $M_{\alpha\beta}$ and $M_{\gamma\gamma}$ are obtained by solving the Schrödinger equations in a pseudopotential scheme,

$$\left[-\frac{1}{2}\nabla^2 + V_{\rm ps}(\mathbf{r})\right]\psi_i(\mathbf{r}) = \epsilon_i\psi_i(\mathbf{r}), \tag{1}$$

where the total electron-ion potential $V_{\rm ps}(\mathbf{r})$ is a superposition of local, screened atomic pseudopotentials $v_\alpha(\mathbf{r})$ and a nonlocal spin-orbit potential $V_{\rm so}$—i.e., $V_{\rm ps}(\mathbf{r})=\Sigma_{n,\alpha}v_\alpha(\mathbf{r}-\mathbf{R}_{n,\alpha})+V_{\rm so}$. The atomic position $\{\mathbf{R}_{n,\alpha}\}$ is obtained from minimizing the total bond-bending and bond-stretching energy using the valence force field (VFF) model.[12,13] The atomistic pseudopotentials v_α (α=In, Ga, As) are fitted to the physically important quantities of bulk InAs and GaAs, including band energies, band offsets, effective masses, deformation potentials, alloy bowing parameters, etc.[14] Because for electrons the spin-orbit coupling is extremely small in the InAs/GaAs quantum dots, we ignored this effect. In general, including the spin-orbit coupling effect will introduce a mixture of different total spin states. Equation (1) is solved in the basis of $\{\phi_{m,\vec{\epsilon},\lambda}(\mathbf{k})\}$ of Bloch orbitals of band index m and wave vector $\mathbf{k}$ of material λ (=InAs, GaAs), strained uniformly to strain $\vec{\epsilon}$ following Ref. 15.

The Hamiltonian of interacting electrons can be written as

$$H = \sum_{i\sigma}\epsilon_\alpha\hat{\psi}^\dagger_{i\sigma}\hat{\psi}_{i\sigma} + \frac{1}{2}\sum_{ijkl}\sum_{\sigma,\sigma'}\Gamma^{i,j}_{k,l}\hat{\psi}^\dagger_{i\sigma}\hat{\psi}^\dagger_{j\sigma'}\hat{\psi}_{k\sigma'}\hat{\psi}_{l\sigma}, \tag{2}$$

where $\hat{\psi}_{i\sigma}(\mathbf{r})=c_{i\sigma}\psi_{i\sigma}(\mathbf{r})$ is the field operator, whereas $c_{i\sigma}$ is a fermion operator. $\psi_i=\sigma_u,\sigma_g,\pi_u,\pi_g$ are the single-particle eigenfunctions of the *ith molecular orbital*, and σ, $\sigma'=1,2$ are spin indices. The Γ^{ij}_{kl} are the Coulomb integrals between molecular orbitals ψ_i, ψ_j, ψ_k, and ψ_l,

$$\Gamma^{ij}_{kl} = \int\int d\mathbf{r}d\mathbf{r}'\frac{\psi^*_i(\mathbf{r})\psi^*_j(\mathbf{r}')\psi_k(\mathbf{r}')\psi_l(\mathbf{r})}{\epsilon(\mathbf{r}-\mathbf{r}')|\mathbf{r}-\mathbf{r}'|}. \tag{3}$$

The $J_{ij}=\Gamma^{ij}_{ji}$ and $K_{ij}=\Gamma^{ij}_{ij}$ are diagonal Coulomb and exchange integrals, respectively. The remaining terms are called off-diagonal or scattering terms. All Coulomb integrals are calculated numerically from atomistic wave functions.[16] We use a phenomenological, position-dependent dielectric function $\epsilon(\mathbf{r}-\mathbf{r}')$ to screen the electron-electron interaction.[16] The many-particle problem of Eq. (2) is solved via the CI method, by expanding the N-electron wave function in a set of Slater determinants, $|\Phi_{e_1,e_2,\ldots,e_N}\rangle=c^\dagger_{e_1}c^\dagger_{e_2}\cdots c^\dagger_{e_N}|\Phi_0\rangle$, where $c^\dagger_{e_i}$ creates an electron in the state e_i. The νth many-particle wave function is then the linear combinations of the determinants,

$$|\Psi_\nu\rangle = \sum_{e_1,e_2,\ldots,e_N}A_\nu(e_1,e_2,\ldots,e_N)|\Phi_{e_1,e_2,\ldots,e_N}\rangle. \tag{4}$$

For the two-electron problems, our calculations include all possible Slater determinants of six confined molecular orbitals.

III. BASIC ELECTRONIC STRUCTURES AT THE SINGLE-PARTICLE LEVEL

A. Double-dot molecular orbitals

We first show the electronic structure of isolated dots α and β. The single-dot electron s and p levels of dots α and β are shown in the right panel of Fig. 2. We see that the s-p energy spacing of dot α is $\epsilon(p_\alpha)-\epsilon(s_\alpha)=52$ meV and that of dot β is $\epsilon(p_\beta)-\epsilon(s_\beta)=59$ meV, compared to 54 meV of dot γ (not shown). The energy level of s_β is slightly (~6 meV) higher than s_α, because dot β is smaller than dot α and therefore has larger confinement. The p levels of all dots have a small energy splitting due to the underlying atomistic symmetry—e.g., $\delta\epsilon(p_\alpha)=6$ meV and $\delta\epsilon(p_\beta)=1$ meV. We further calculated the fundamental exciton energy of dot α, $E_X(\alpha)=1153$ meV, and that of dot β, $E_X(\beta)=1159$ meV. The energy difference in exciton of dots α and β is about 6 meV, in agreement with experiment.[10] The fundamental exciton

energy of the "averaged" dot γ is $E_X(\gamma)=1156$ meV.

When two dots α and β couple, the bonding and antibonding "molecular orbitals" ensue from the single-dot orbitals. The energy levels of molecular orbitals are shown in the left panel of Fig. 2. We show the single-particle levels of molecular orbitals[8,9] σ_g and σ_u originating from s orbitals and π_u and π_g originating from p orbitals. The bonding and antibonding splittings $\Delta_\sigma=\epsilon(\sigma_u)-\epsilon(\sigma_g)$ and $\Delta_\pi=\epsilon(\pi_g)-\epsilon(\pi_u)$ increase with the decrease of interdot distance, because the coupling between the top and bottom dots gets stronger. This picture is similar to what we obtained for homo-QDM's. However, there is an important difference between the homo-QDM's $M_{\gamma\gamma}$ and hetero-QDM's $M_{\alpha\beta}$: in the former case, the bonding and antibonding splittings Δ_σ and Δ_π decay to almost zero at large interdot distance, while in the later case, Δ_σ and Δ_π tend to constants ($\Delta_\sigma\sim 7$ meV, $\Delta_\pi\sim 10$ meV here), because the molecular orbitals gradually convert at large interdot distance to single-dot energy levels—e.g., the σ_g levels convert to top-dot s orbitals and σ_u convert to bottom-dot s orbitals; therefore, the energy splitting between the first and second molecular states at large distances is approximately the energy difference between the s orbitals of the top and bottom dots—i.e., $\Delta_\sigma\sim\epsilon(s_\beta)-\epsilon(s_\alpha)\neq 0$ for $M_{\alpha\beta}$.

Figure 2 shows that at interdot distance $d=10$ nm, the molecular orbital levels are about 25 meV higher than the isolated dot levels, although the direct electronic coupling between two dots is much smaller than this quantity. This energy shift results from the long-range strain effects experienced by one dot due to the presence of the second dots. This effect is missed in effective-mass-approximation- (EMA-) type model calculations,[17] which ignore strain effects.

B. Single-dot-localized orbitals

The above discussions pertain to the basis of double-dot molecular orbitals. An alternative way to study QDM's is to use a dot-localized basis. We have demonstrated[8,9] that dot-localized orbitals can be a useful tool to analyze the QDM physics, including electron double occupation and two-electron entanglement.

Dot-localized orbitals χ_η can be obtained from a unitary rotation of molecular orbitals—i.e.,

$$\chi_\eta=\sum_{i=1}^{N}\mathcal{U}_{\eta,i}\psi_i, \tag{5}$$

where ψ_i is the ith molecular orbital and $\mathcal{U}$ is a unitary matrix—i.e., $\mathcal{U}^\dagger\mathcal{U}=I$. We choose the unitary matrices $\mathcal{U}$ that maximize the total orbital self-Coulomb energy.[9,18] The procedure of finding $\mathcal{U}$ is described in Appendix B of Ref. 9. As we will show below these dot-localized orbitals χ_η have the advantage of being only weakly dependent on the interdot coupling. This invariance may provide simplified pictures for a qualitative understanding of the QDM physics.

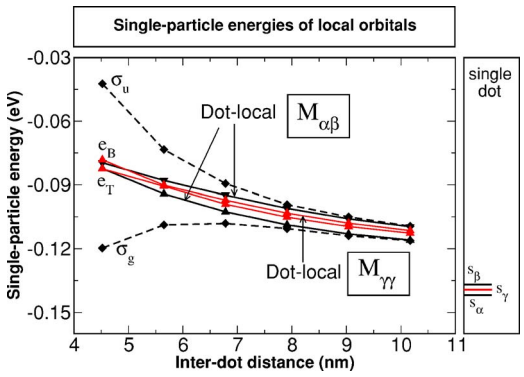

FIG. 3. (Color online) Left panel: the energy levels of dot-localized orbitals for QDM's $M_{\alpha\beta}$ (black solid lines) and $M_{\gamma\gamma}$ (red solid lines). e_T and e_B denote the s orbitals of the top and bottom dots, respectively. The molecular orbitals energy levels σ_g and σ_u (dashed lines) are shown for dot molecules $M_{\alpha\beta}$. Right panel: s levels of *isolated* dots α, β, and γ.

1. Single-particle energies of dot-localized orbitals

The single-particle levels of dot-localized orbitals and the hopping (or tunneling) term between two dots can be obtained from

$$e_\eta=\langle\chi_\eta|\hat{H}_0|\chi_\eta\rangle=\sum_i\mathcal{U}^*_{\eta,i}\mathcal{U}_{\eta,i}\epsilon_i, \tag{6}$$

$$t_{\eta_1\eta_2}=\langle\chi_{\eta_1}|\hat{H}_0|\chi_{\eta_2}\rangle=\sum_i\mathcal{U}^*_{\eta_1,i}U_{\eta_2,i}\epsilon_i, \tag{7}$$

where ϵ_i is the single-particle energy of the ith molecular orbital and $\hat{H}_0=\Sigma_{i\sigma}\epsilon_\alpha\hat{\psi}^\dagger_{i\sigma}\hat{\psi}_{i\sigma}$ is the single-particle Hamiltonian. Figure 3 depicts the single-particle levels e_T and e_B of the dot-localized orbitals of both top and bottom dots for interdot distances d in the range from 4 nm to 10 nm. (Here, we denote the top dot T and the bottom dot B, to distinguish them from isolated dots α, β, and γ.) e_T and e_B of $M_{\alpha\beta}$ are shown as the black solid lines, and those of $M_{\gamma\gamma}$ are shown as the red solid lines. At large d, the energy difference $e_B-e_T\sim 6$ meV for $M_{\alpha\beta}$ is close to the value of the difference $\epsilon(s_\beta)-\epsilon(s_\alpha)$ between s orbitals of isolated dots α and β. This energy difference gets smaller when the two dots move closer, because the energy levels of the top dot rise faster than those of the bottom dots due to the strain asymmetry. For the homo-QDM's $M_{\gamma\gamma}$, e_T and e_B are almost degenerate. The small difference (~ 1 meV) between them is due to strain and alloy effects. We also plot in Fig. 3 the energies of the molecular orbitals σ_u and σ_g as dashed lines for $M_{\alpha\beta}$. As we see, for $d>9$ nm, the dot-localized state e_B of $M_{\alpha\beta}$ is almost identical to the molecular orbital σ_u, while e_T merges with σ_g, indicating that at large d, molecular orbitals convert to dot-centered orbitals for $M_{\alpha\beta}$.

The quantity $2t$ measures the coupling strength between the top and bottom dots, and directly determines the two-electron properties such as singlet-triplet splitting in the QDM. We calculate this hopping energy between the s orbitals of top and bottom dots at different interdot distances for both $M_{\alpha\beta}$ and $M_{\gamma\gamma}$ in Fig. 4. (We ignore the orbital index s to

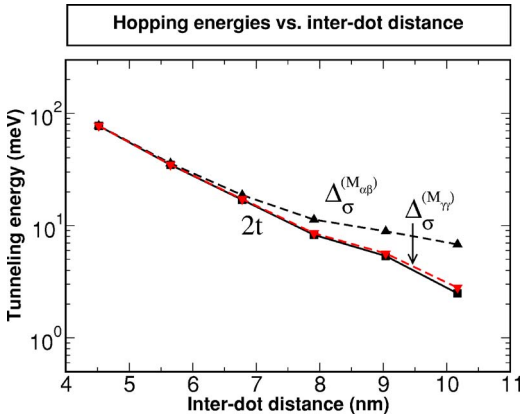

FIG. 4. (Color online) The interdot hopping energy $2t$ (solid lines) of hetero-QDM $M_{\alpha\beta}$ and homo-QDM $M_{\gamma\gamma}$. We also show the bonding-antibonding splitting Δ_σ of $M_{\alpha\beta}$ and $M_{\gamma\gamma}$.

simplify the notation.) We find that $2t(M_{\alpha\beta})$ and $2t(M_{\gamma\gamma})$ are almost identical at all interdot distances. However, the hopping energies calculated here are much larger than we obtained for the pure InAs/GaAs QDM,[9] because the alloy QDM's have much smaller energy barrier between two dots than pure QDM's. In general, the quantity $2t$ does not equal the bonding-antibonding splitting $\Delta_\sigma=\sqrt{\delta^2+4t^2}$, where $\delta=\epsilon(e_T)-\epsilon(e_B)$, being the energy difference of s orbitals of the top and bottom dots. For homo-QDM's, where $\delta/2t\ll 1$, we have $2t\sim\Delta_\sigma$ as seen in Fig. 4. However, for hetero-QDM's, Δ_σ may be significantly different from $2t$, especially at *large* interdot distances, where $\delta/2t\gg 1$, also illustrated in Fig. 4. Experimentally,[19] one usually measures the bonding-antibonding splitting rather than the hopping $2t$. Therefore, to get the hopping energy between two dots, one needs to know the energy difference δ of two dots.

2. Coulomb integrals of dot-localized orbitals

The Coulomb integrals in the dot-localized basis can be obtained from Coulomb integrals of molecular orbitals as follows:

$$\tilde{\Gamma}^{\eta_1,\eta_2}_{\eta_3,\eta_4}=\sum_{i,j,k,l}\mathcal{U}^*_{\eta_1,i}\mathcal{U}^*_{\eta_2,j}\mathcal{U}_{\eta_3,k}\mathcal{U}_{\eta_4,l}\Gamma^{i,j}_{k,l}, \tag{8}$$

where $\Gamma^{i,j}_{k,l}$ are the Coulomb integrals in the molecular basis. The direct Coulomb integrals J_{TT}, J_{BB}, and J_{TB} for $M_{\alpha\beta}$ are shown in Fig. 5. The Coulomb integrals $J_{TT}\sim J_{\alpha\alpha}=21.4$ meV and $J_{BB}\sim J_{\beta\beta}=22.3$ meV are almost constants at all interdot distances, suggesting that the dot-localized orbitals are approximately unchanged for different interdot distances d. $J_{\beta\beta}>J_{\alpha\alpha}$, as dot β is smaller than dot α. The interdot Coulomb interaction J_{TB} decays slowly as $1/d$. The exchange energies (not shown) between the top and bottom electrons is orders of magnitude smaller than the hopping energy and therefore can be ignored in practice. For the homo-QDM $M_{\gamma\gamma}$, we found that on-site Coulomb energies $J_{TT}\sim J_{BB}$, are both very close to the average values of J_{TT} and J_{BB} of $M_{\alpha\beta}$. The interdot Coulomb energies J_{TB} of $M_{\alpha\beta}$ and $M_{\gamma\gamma}$ are also extremely close.

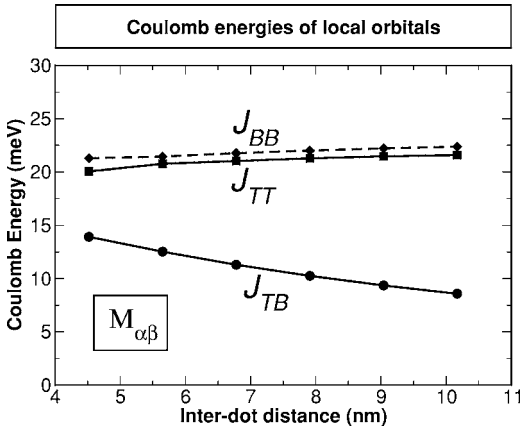

FIG. 5. The Coulomb energies of dot-localized orbitals of hetero-QDM $M_{\alpha\beta}$. J_{TT} and J_{BB} are the s orbital self-Coulomb energies of top and bottom dots, respectively, whereas J_{TB} are the Coulomb energies between s orbitals of the top and bottom dots.

IV. TWO ELECTRONS IN THE DOT MOLECULE

A. Many-body energy states

The two-electron-in-a-QDM problem is of special interest, as it is the prototype of a quantum gate using QDM's.[4] We calculate the two-electron energy levels by the configuration interaction method using Slater determinants constructed from confined molecular orbitals σ_g, σ_u and π_u, π_g, which give 66 configurations in total. The two-electron energies Σ and $^3\Pi_u$ for hetero-QDM's $M_{\alpha\beta}$ are plotted in Fig. 6(a). To compare with homo-QDM's, we show the two-

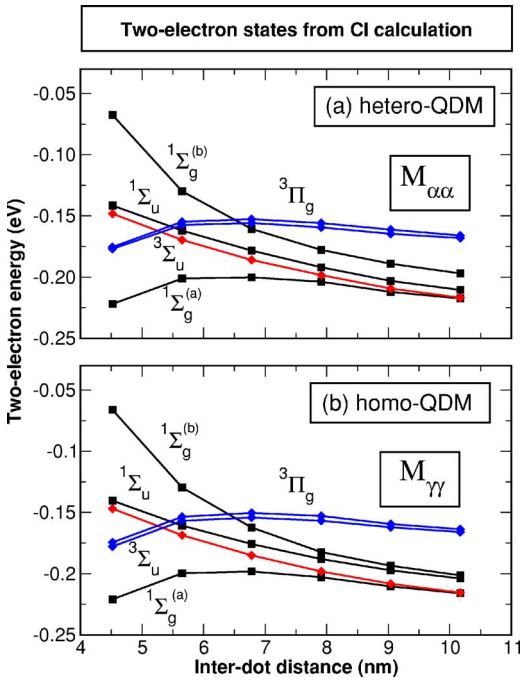

FIG. 6. (Color online) Two-electron states for (a) hetero-QDM $M_{\alpha\beta}$ and (b) homo-QDM $M_{\gamma\gamma}$, including the singlet $^1\Sigma_g^{(a)}$, $^1\Sigma_u$, and $^1\Sigma_g^{(b)}$ states and the threefold-degenerated triplet states $^3\Sigma_u$ as well as two threefold-degenerated triplet states $^3\Pi_u$.

electron states of $M_{\gamma\gamma}$ in Fig. 6(b). The energy levels of $M_{\alpha\beta}$ are similar to those of $M_{\gamma\gamma}$, in the following way: (i) The order of the CI levels is unchanged; particularly, the ground states are still the singlet states ${}^1\Sigma_g^{(a)}$ at all interdot distances; (ii) the trend of each CI level versus interdot distance d is similar to what we obtained for $M_{\gamma\gamma}$. There are also some differences between the hetero-QDM's $M_{\alpha\beta}$ and homo-QDM's $M_{\gamma\gamma}$, especially at larger interdot distances. For example, in the homopolar QDM's, the ${}^1\Sigma_u$ state is almost degenerate with ${}^1\Sigma_g^{(b)}$ at large interdot distance, while in $M_{\alpha\beta}$, ${}^1\Sigma_g^{(b)}$ is about 13 meV higher than ${}^1\Sigma_u$ at $d=10$ nm. At large d, ${}^1\Sigma_u$ and ${}^1\Sigma_g^{(b)}$ correspond to the states that two electrons localize on the same dots.[8,9] The energy difference between ${}^1\Sigma_g^{(b)}$ and ${}^1\Sigma_u$ is due to the size difference of dots α and β.

The singlet ${}^1\Sigma_g^{(a)}$ and triplet states ${}^3\Sigma$ can be used as two-qubit states in quantum computing. In a proposed quantum SWAP gate,[4] the gate operation time $\tau \sim 1/J_{S\text{-}T}$, where $J_{S\text{-}T}$ is the singlet-triplet energy splitting. The singlet-triplet splitting of $M_{\alpha\beta}$ is shown in Fig. 7 on a semilogarithmic plot. We see that it decays approximately exponentially with the interdot distance. We also show in Fig. 7 the singlet-triplet splitting of the homo-QDM $M_{\gamma\gamma}$. We found that the $J_{S\text{-}T}$ of homo-QDM $M_{\gamma\gamma}$ is slightly smaller than the $J_{S\text{-}T}$ of hetero-QDM $M_{\alpha\beta}$, though the hopping energies of $M_{\alpha\beta}$ and $M_{\gamma\gamma}$ are almost identical. In the hetero-QDM case, the singlet wave function has more weight on the lower-energy dot and therefore lowers the singlet energy and increases the singlet-triplet splitting.

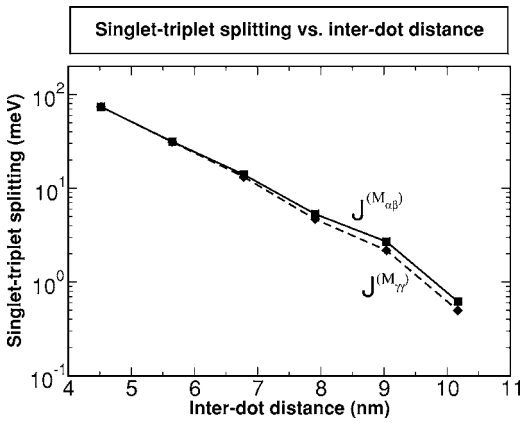

FIG. 7. The singlet-triplet splitting $J_{S\text{-}T}$ vs interdot distance for hetero-QDM $M_{\alpha\beta}$ (solid line) and homo-QDM $M_{\gamma\gamma}$ (dashed line).

B. Double occupation of one of the dots in a QDM

Double occupation means that two electrons occupy the same dot in a QDM. If the double-occupation rate is high, the quantum gate operation may fail. The double-occupation rate also reflects the localization properties of electrons in the QDM. If the double-occupation rate is zero, each dot has one electron, whereas a double-occupation rate of 1 means that two electrons are always localized on a single dot. When the double-occupation rate is 0.5, two electrons are delocalized between two dots. The double occupation can be conveniently analyzed in the dot-localized basis by transforming the CI equations to the dot-localized basis.[8] In the simplest case, we consider only the s orbital for each dot, which gives six configurations as follows: $|e_T^{\uparrow}, e_B^{\uparrow}\rangle$, $|e_T^{\downarrow}, e_B^{\downarrow}\rangle$, $|e_T^{\uparrow}, e_B^{\downarrow}\rangle$, $|e_T^{\downarrow}, e_B^{\uparrow}\rangle$, $|e_B^{\uparrow}, e_B^{\downarrow}\rangle$, and $|e_T^{\uparrow}, e_T^{\downarrow}\rangle$. The Hamiltonian in this basis set is[9]

$$H = \begin{pmatrix} e_T + e_B + J_{TB} - K_{TB} & 0 & 0 & 0 & 0 & 0 \\ 0 & e_T + e_B + J_{TB} - K_{TB} & 0 & 0 & 0 & 0 \\ 0 & 0 & e_T + e_B + J_{TB} & -K_{TB} & t & t \\ 0 & 0 & -K_{TB} & e_T + e_B + J_{TB} & -t & -t \\ 0 & 0 & t & -t & 2e_B + J_{BB} & 0 \\ 0 & 0 & t & -t & 0 & 2e_T + J_{TT} \end{pmatrix}, \tag{9}$$

where $t=t_{TB}$. We ignored in Eq. (9) the off-diagonal Coulomb integrals, which are much smaller than the hopping t.

The calculation of the matrix elements of Eq. (9) is described in Sec. III B. The two electrons can be either both on the top dots or both on the bottom dots, or one on the top and the other on the bottom dot. We denote by $\{|\chi_{l,p}^{\sigma}, \chi_{l',p'}^{\sigma'}\rangle\}$ the configuration where one electron is on the lth orbital of the p dot with spin σ and the other electron is on the (l')th orbital of the p' dot with spin σ'. Then the double-occupation rate $Q_{pp}^{(\nu)}$ in the many-particle state ν is the probability of two electrons occupying the dot, $p=(T \text{ or } B)$ at the same time—i.e.,

$$Q_{pp}^{(\nu)} = \sum_{l\sigma,l'\sigma'} P_\nu(|\chi_{l,p}^{\sigma}, \chi_{l',p}^{\sigma'}\rangle), \tag{10}$$

where $P_\nu(\mathcal{C})$ is the weight of the configuration $\mathcal{C}$ in the many-body wave functions of state ν. The total probability of two electrons being on the *same* dot is then $Q_{\text{tot}}^{(\nu)} = Q_{TT}^{(\nu)} + Q_{BB}^{(\nu)}$ for the νth state.

We plot Q_{tot}, Q_{TT}, and Q_{BB} of state ${}^1\Sigma_g^{(a)}$ for $M_{\alpha\beta}$ in Fig. 8(a) and for $M_{\gamma\gamma}$ in Fig. 8(b). We also performed calculations

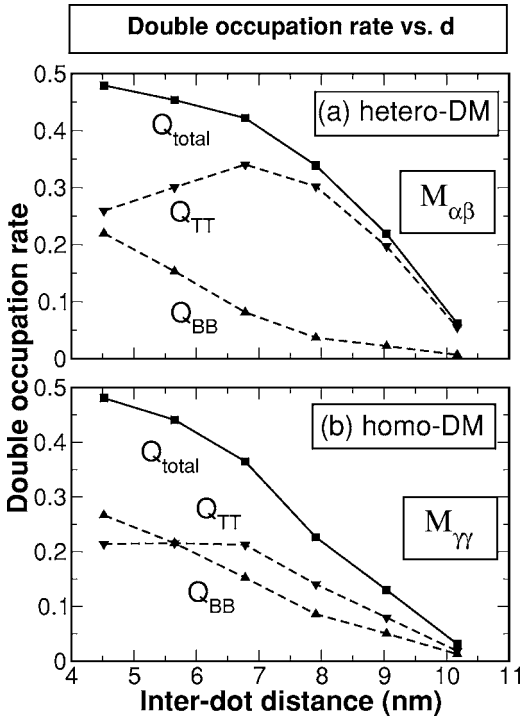

FIG. 8. The double-occupation rate of the ground-state singlet ${}^1\Sigma_g^{(a)}$ vs interdot distance for (a) hetero-QDM $M_{\alpha\beta}$ and (b) homo-QDM $M_{\gamma\gamma}$.

on a "symmetrized" model QDM $M_{\alpha'\alpha'}$ by setting $e'_T=e'_B=(e_T+e_B)/2$ and $J'_{TT}=J'_{BB}=(J_{TT}+J_{BB})/2$ of $M_{\alpha\beta}$ in Eq. (9). $M_{\alpha'\alpha'}$ represents an *ideal* homo-QDM, without the asymmetry caused by strain, size, and alloy composition effects. When compare the double occupation of the hetero- and homo-QDM's, we see that (i) for both types of QDM's, $Q_{\text{tot}}\sim 0.5$ at $d\sim 4.5$ nm, meaning that two electrons are delocalized on two dots. For both QDM's, Q_{tot} decays monotonically with the interdot distance, and at $d\sim 10$ nm, $Q_{\text{tot}}\sim 0$, meaning that the two electrons are about each localized on one of the two dots.

On the other hand, the double occupation of individual dots Q_{TT} and Q_{BB} differs substantially for homo-QDM's and hetero-QDM's: (ii) For the homo-QDM $M_{\alpha'\alpha'}$, $Q_{BB}=Q_{TT}$ and decay monotonically with the interdot distances. Q_{BB} and Q_{TT} of $M_{\gamma\gamma}$ have similar features, although Q_{BB} is slightly different from Q_{TT} due to strain and alloy effects. This feature is also seen in the homo-QDM made of pure InAs/GaAs dots.[8,9] In the hetero-QDM's $M_{\alpha\beta}$, Q_{TT} behaves very differently from Q_{BB} because the effective single-particle energy $e_T<e_B$. Whereas Q_{BB} decays monotonically with the interdot distance, Q_{TT} has a maximum at $d\sim 7$ nm. The reason is that at $d\sim 4.5$ nm, the hopping energy $2t$ is much larger than e_B-e_T; therefore, the electrons can overcome the energy barrier between the top and bottom dots and distribute evenly between two dots, leading to $Q_{TT}\sim Q_{BB}$. At larger d, $2t\ll e_B-e_T$, and the electrons would prefer to localize on the top dots, leading to $Q_{TT}\gg Q_{BB}$. Therefore, even when the total double-occupation rate drops down, Q_{TT} still increases and reaches the maximum at $d=7$ nm. For $d>7$ nm, Q_{TT} decays as Q_{tot} decays.

(iii) The homo-QDM's $M_{\alpha'\alpha'}$ and $M_{\gamma\gamma}$ have almost the same *total* double occupation, both smaller than that of the hetero-QDM $M_{\alpha\beta}$. The asymmetry between two dots increases the total double occupation. In an extreme case, where $e_T\ll e_B$, the two electrons could always localize on the top dots, leading to $Q_{\text{tot}}=Q_{TT}=1$.

V. ENTANGLEMENT

A. Degree of entanglement for two electrons

The degree of entanglement (DOE) is one of the most important quantities for successful quantum gate operations. For *distinguishable* particles such as an electron and a hole, the DOE can be calculated from the von Neumann entropy formulation.[20–23] However, the von Neumann entropy formulation cannot be used directly to calculate the DOE for *indistinguishable* particles.[24–30] Schliemann *et al.* proposed a quantum correlation function for two electrons which has similar properties as the DOE.[24] However, the generalization of this quantum correlation function to a system that has more than two single-particle levels is complicated. We proposed a DOE measure[9] for indistinguishable fermions using Slater decompositions[24,31] as

$$\mathcal{S}=-\sum_u z_i^2\log_2 z_i^2, \tag{11}$$

where z_i are Slater decomposition coefficients and $\Sigma_i z_i^2=1$. As shown in Ref. 9, the DOE measure, Eq. (11), reduces to the usual von Neumann entropy for *distinguishable* particles when the two electrons are far from each other. In Refs. 25 and 26, a similar DOE measure was defined, which, however, due to a different normalization condition for z_i being used, does not reduce to the usual von Neumann entropy even when the two electrons can be distinguished by their sites.

The DOE of Σ states calculated from Eq. (11) for the hetero-QDM $M_{\alpha\beta}$, the homo-QDM $M_{\gamma\gamma}$, and the model homo-QDM $M_{\alpha'\alpha'}$ are shown in Figs. 9(a)–9(c), respectively. All of the three QDM's have the following features: (i) $\mathcal{S}({}^1\Sigma_g^{(a)})$ is close to zero (unentangled) at $d\sim 4.5$ nm and close to unity (fully entangled) at $d\sim 10$ nm. (ii) $\mathcal{S}({}^3_0\Sigma)$ is almost unity (fully entangled) at all interdot distances. However, $\mathcal{S}({}^1\Sigma_g^{(a)})$ of the homo-QDM $M_{\gamma\gamma}$ [which is very close to the $\mathcal{S}({}^1\Sigma_g^{(a)})$ of $M_{\alpha'\alpha'}$] is larger than $\mathcal{S}({}^1\Sigma_g^{(a)})$ of the hetero-QDM $M_{\alpha\beta}$, showing that the asymmetry in a QDM lowers the two-electron entanglement of the ground-state singlet.

In contrast to $\mathcal{S}({}^1\Sigma_g^{(a)})$ and $\mathcal{S}({}^3_0\Sigma)$, $\mathcal{S}({}^1\Sigma_g^{(b)})$ and $\mathcal{S}({}^1\Sigma_u)$ are very sensitive to the asymmetry of the QDM's. In general, if the two dots have identical electronic structures (e.g., in the simple Hubbard model), $\mathcal{S}({}^1\Sigma_g^{(b)})=\mathcal{S}({}^1\Sigma_g^{(a)})$ and $\mathcal{S}({}^1\Sigma_u)=1$,[9] as illustrated in Fig. 9(c) for $M_{\alpha'\alpha'}$. For $M_{\gamma\gamma}$, which is somehow asymmetric due to strain and alloy effects, $\mathcal{S}({}^1\Sigma_g^{(b)})$ is close to $\mathcal{S}({}^1\Sigma_g^{(a)})$ at small d and drops down at large d, whereas for $M_{\alpha\beta}$, $\mathcal{S}({}^1\Sigma_g^{(b)})$ is different from $\mathcal{S}({}^1\Sigma_g^{(a)})$ at all interdot distances. The slight asymmetry in $M_{\gamma\gamma}$ also causes $\mathcal{S}({}^1\Sigma_u)$ to drop down at large d, similar to $\mathcal{S}({}^1\Sigma_u)$ of $M_{\alpha\beta}$.

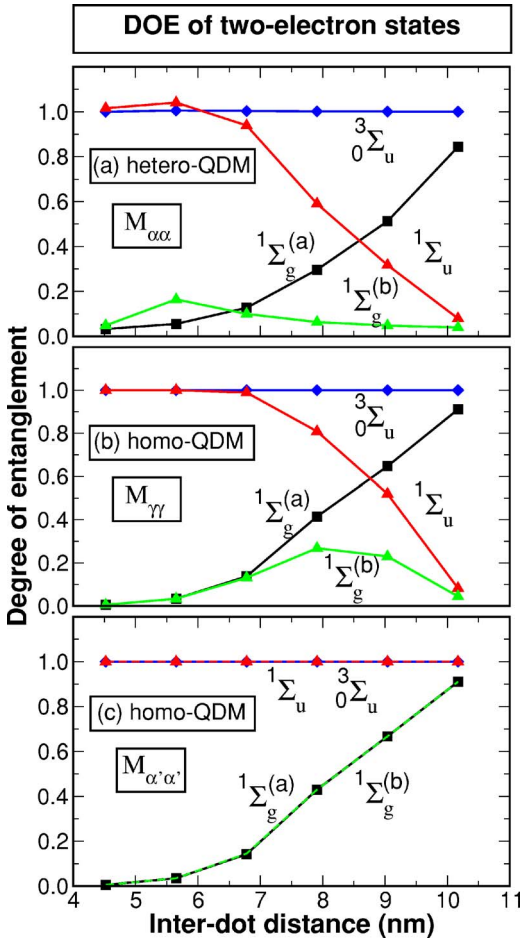

FIG. 9. (Color online) The degree of entanglement of two-electron states $^1\Sigma_g^{(a)}$, $^1\Sigma_u$, $^1\Sigma_g^{(b)}$, and $^3\Sigma_u$, in (a) the hetero-QDM $M_{\alpha\beta}$, (b) the homo-QDM $M_{\gamma\gamma}$, and (c) the model-"symmetrized" homo-QDM $M_{\alpha'\alpha'}$.

B. Degree of entanglement vs double occupation

Experimentally, it is very hard to measure the DOE of two electrons in the QDM directly, while it is relatively easy to measure the possibility of double occupation. Therefore it would be useful to explore the relation between the DOE and the double-occupation rate. The triplet states $^3\Sigma$ have negligible double-occupation rate due to the Pauli exclusion principle. Here, we discuss the relation between the DOE and double-occupation rate for the ground-state singlet $^1\Sigma_g^{(a)}$. We consider the simplest case, where only the s orbital in each dot is considered. The ground-state singlet $^1\Sigma_g^{(a)}$ wave function can be generally written as

$$\Psi(^1\Sigma_g^{(a)}) = c_1|e_T^{\uparrow}, e_B^{\downarrow}\rangle + c_2|e_B^{\uparrow}, e_T^{\downarrow}\rangle + c_3|e_T^{\uparrow}, e_T^{\downarrow}\rangle + c_4|e_B^{\uparrow}, e_B^{\downarrow}\rangle \tag{12}$$

and $|c_1|^2+|c_2|^2+|c_3|^2+|c_4|^2=1$. Alternatively, we have

$$\Psi(^1\Sigma_g^{(a)}) = \sum_{i,j} \omega_{ij}|i\rangle \otimes |j\rangle, \tag{13}$$

where

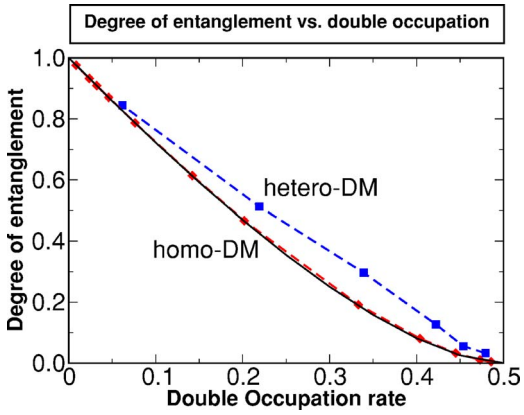

FIG. 10. (Color online) Comparison of the degree of entanglement vs double-occupation rate for hetero- and homo-QDM's. The black solid line represents the analytical results of the homo-QDM, and the red dashed line represents the numerical results for the homo-QDM's $M_{\alpha'\alpha'}$ and $M_{\gamma\gamma}$ whereas the blue line represents the results for hetero-QDM's $M_{\alpha\beta}$.

$$\omega = \begin{pmatrix} 0 & -c_3 & 0 & -c_1 \\ c_3 & 0 & c_2 & 0 \\ 0 & -c_2 & 0 & -c_4 \\ c_1 & 0 & c_4 & 0 \end{pmatrix} \tag{14}$$

and $|i\rangle, |j\rangle = |e_T^{\uparrow}\rangle, |e_T^{\downarrow}\rangle, |e_B^{\uparrow}\rangle, |e_B^{\downarrow}\rangle$. We can use Eq. (11) to calculate the DOE, where $z_1^2 = \frac{1}{2}[1-\sqrt{1-4(c_1c_2-c_3c_4)^2}]$ and $z_2^2 = \frac{1}{2}[1+\sqrt{1-4(c_1c_2-c_3c_4)^2}]$ are the eigenvalues of $\omega^{\dagger}\omega$. For a QDM with reflection symmetry, we have $c_1=c_2$ and $c_3=c_4$, and therefore $z_1^2=\frac{1}{2}[1-\sqrt{1-(1-4c_3^2)^2}]$ and $z_2^2=\frac{1}{2}[1+\sqrt{1-(1-4c_3^2)^2}]$. Using the definition of double-occupation rate, $Q_{\text{tot}}=c_3^2+c_4^2$, we have

$$z_1^2 = \tfrac{1}{2}[1-\sqrt{1-(1-2Q_{\text{tot}})^2}],$$

$$z_2^2 = \tfrac{1}{2}[1+\sqrt{1-(1-2Q_{\text{tot}})^2}]. \tag{15}$$

The DOE of $^1\Sigma_g^{(a)}$ is calculated by substituting z_1^2 and z_2^2 into Eq. (11). We plot the DOE versus double-occupation rate of the above ideal model in Fig. 10 as a black solid line. We also present in the same figure the DOE of $M_{\alpha\beta}$, $M_{\gamma\gamma}$, and $M_{\alpha'\alpha'}$ versus the double-occupation rate. We found that the double-occupation dependence of the DOE for the homo-QDM $M_{\alpha'\alpha'}$ has perfect agreement with the analytical result, which is also true for $M_{\gamma\gamma}$ even though it has small asymmetry in the molecule due to the strain and alloy effects. We also checked the homo-QDM made of pure InAs/GaAs dots[8,9] and found the same double-occupation dependence of the DOE for the $^1\Sigma_g^{(a)}$ state, indicating this is a robust feature for homo-QDM's. However, the double-occupation dependence of the DOE for $M_{\alpha\beta}$ deviates from the ideal case because dots α and β are different.

VI. SUMMARY

We have studied the electronic structures of quantum dot molecules made of (In,Ga)As/GaAs dots of different sizes

(hetero-QDM's) and compared them to that of quantum dot molecules made of identical dots (homo-QDM's). We found that while the hetero-QDM's and homo-QDM's have relatively similar electronic structures at short interdot distance, they differ significantly at large interdot distance. (i) Unlike those of homo-QDM's, the single-particle molecular orbitals of hetero-QDM's convert to dot-localized orbitals at large interdot distance. (ii) Consequently, the bonding-antibonding splitting of molecular orbitals is significantly larger than the electron hopping energy in a hetero-QMD at large interdot distance, whereas for homo-QDM's, the bonding-antibonding splitting is very similar to the hopping energy. (iii) The asymmetry of the QDM will significantly increase the double occupation for the two-electron ground states and therefore lower the degree of entanglement of the two electrons.

ACKNOWLEDGMENTS

L.H. acknowledges support from the Chinese National Fundamental Research Program, the Innovation Funds and "Hundreds of Talents" program from the Chinese Academy of Sciences, and the National Natural Science Foundation of China (Grant No. 10674124). The work done at NREL was funded by the U.S. Department of Energy, Office of Science, Basic Energy Science, Materials Sciences and Engineering, LAB-17 initiative, under Contract No. DE-AC36-99GO10337 to NREL.

[1] Q. Xie, A. Madhukar, P. Chen, and N. P. Kobayashi, Phys. Rev. Lett. **75**, 2542 (1995).
[2] G. S. Solomon, J. A. Trezza, A. F. Marshall, and J. S. Harris, Phys. Rev. Lett. **76**, 952 (1996).
[3] M. Bayer, P. Hawrylak, K. Hinzer, S. Fafard, M. Korkusinski, Z. R. Wasilewski, O. Stern, and A. Forchel1, Science **291**, 451 (2001).
[4] D. Loss and D. P. DiVincenzo, Phys. Rev. A **57**, 120 (1998).
[5] J. R. Petta, A. C. Johnson, C. M. Marcus, M. P. Hanson, and A. C. Gossard, Phys. Rev. Lett. **93**, 186802 (2004).
[6] A. C. Johnson, J. R. Petta, C. M. Marcus, M. P. Hanson, and A. C. Gossard, Phys. Rev. B **72**, 165308 (2005).
[7] G. Bester, J. Shumway, and A. Zunger, Phys. Rev. Lett. **93**, 047401 (2004).
[8] L. He, G. Bester, and A. Zunger, Phys. Rev. B **72**, 081311(R) (2005).
[9] L. He, G. Bester, and A. Zunger, Phys. Rev. B **72**, 195307 (2005).
[10] M. C. Bödefeld, R. J. Warburton, K. Karrai, J. P. Kotthaus, G. Medeiros-Ribeiro, and P. M. Petroff, Appl. Phys. Lett. **74**, 1839 (1999).
[11] E. A. Stinaff, M. Scheibner, A. S. Bracker, I. V. Ponomarev, V. L. Korenev, M. E. Ware, M. F. Doty, T. L. Reinecke, and D. Gammon, Science **311**, 636 (2006).
[12] P. N. Keating, Phys. Rev. **145**, 637 (1966).
[13] J. L. Martins and A. Zunger, Phys. Rev. B **30**, R6217 (1984).
[14] A. J. Williamson, L.-W. Wang, and A. Zunger, Phys. Rev. B **62**, 12963 (2000).
[15] L.-W. Wang and A. Zunger, Phys. Rev. B **59**, 15806 (1999).
[16] A. Franceschetti, H. Fu, L.-W. Wang, and A. Zunger, Phys. Rev. B **60**, 1819 (1999).
[17] M. Rontani, F. Troiani, U. Hohenester, and E. Molinari, Solid State Commun. **119**, 309 (2001).
[18] C. Edmiston and K. Ruedenberg, Rev. Mod. Phys. **35**, 457 (1963).
[19] T. Ota, M. Rontani, S. Tarucha, Y. Nakata, H. Z. Song, T. Miyazawa, T. Usuki, M. Takatsu, and N. Yokoyama, Phys. Rev. Lett. **95**, 236801 (2005).
[20] M. A. Nielsen and I. L. Chuang, *Quantum Computation and Quantum Information* (Cambridge University Press, Cambridge, England, 2000).
[21] C. H. Bennett, H. J. Bernstein, S. Popescu, and B. Schumacher, Phys. Rev. A **53**, 2046 (1996).
[22] C. H. Bennett, D. P. DiVincenzo, J. A. Smolin, and W. K. Wootters, Phys. Rev. A **54**, 3824 (1996).
[23] A. Wehrl, Rev. Mod. Phys. **50**, 221 (1978).
[24] J. Schliemann, J. I. Cirac, M. Kuś, M. Lewenstein, and D. Loss, Phys. Rev. A **64**, 022303 (2001).
[25] R. Paskauskas and L. You, Phys. Rev. A **64**, 042310 (2001).
[26] Y. S. Li, B. Zeng, X. S. Liu, and G. L. Long, Phys. Rev. A **64**, 054302 (2001).
[27] P. Zanardi, Phys. Rev. A **65**, 042101 (2002).
[28] Y. Shi, Phys. Rev. A **67**, 024301 (2003).
[29] H. M. Wiseman and J. A. Vaccaro, Phys. Rev. Lett. **91**, 097902 (2003).
[30] G. C. Ghirardi and L. Marinatto, Phys. Rev. A **70**, 012109 (2004).
[31] C. N. Yang, Rev. Mod. Phys. **34**, 694 (1962).